Published in final edited form as:

Biochemistry. 2010 January 12; 49(1): 68–77. doi:10.1021/bi9016022.

Control of Integrin $\alpha_{IIb}\beta_3$ Outside-In Signaling and Platelet Adhesion by Sensing the Physical Properties of Fibrin(ogen) Substrates[†]

Nataly P. Podolnikova[‡], **Ivan S. Yermolenko**[‡], **Alexander Fuhrmann**[||], **Valeryi K. Lishko**[‡], **Sergei Magonov**[⊥], **Benjamin Bowen**[§], **Joerg Enderlein**[#], **Andriy V. Podolnikov**[‡], **Robert Ros**[||], and **Tatiana P. Ugarova**[‡,*]

[‡]Center for Metabolic Biology, Arizona State University, Tempe, Arizona 85287

[§]Department of Bioengineering, Arizona State University, Tempe, Arizona 85287

[||]Department of Physics, Arizona State University, Tempe, Arizona 85287

[⊥]Agilent Technologies, Chandler, Arizona 85226

[#]Third Institute of Physics, George August University Göttingen, 37077 Göttingen, Germany

Abstract

The physical properties of substrates are known to control cell adhesion via integrin-mediated signaling. Fibrin and fibrinogen, the principal components of hemostatic and pathological thrombi, may represent biologically relevant substrates whose variable physical properties control adhesion of leukocytes and platelets. In our previous work, we have shown that binding of fibrinogen to the surface of fibrin clot prevents cell adhesion by creating an antiadhesive fibrinogen layer. Furthermore, fibrinogen immobilized on various surfaces at high density supports weak cell adhesion whereas at low density it is highly adhesive. To explore the mechanism underlying differential cell adhesion, we examined the structural and physical properties of surfaces prepared by deposition of various concentrations of fibrinogen using atomic force microscopy and force spectroscopy. Fibrinogen deposition at high density resulted in an aggregated multilayered material characterized by low adhesion forces. In contrast, immobilization of fibrinogen at low density produced a single layer in which molecules were directly attached to the solid surface, resulting in higher adhesion forces. Consistent with their distinct physical properties, low- but not high-density fibrinogen induced strong $\alpha_{IIb}\beta_3$-mediated outside-in signaling in platelets, resulting in their spreading. Moreover, while intact fibrin gels induced strong signaling in platelets, deposition of fibrinogen on the surface of fibrin resulted in diminished cell signaling. The data suggest that deposition of a multilayered fibrinogen matrix prevents stable cell adhesion by modifying the physical properties of surfaces, which results in reduced force generation and insufficient signaling. The mechanism whereby circulating fibrinogen alters adhesive properties of fibrin clots may have important implications for control of thrombus formation and thrombogenicity of biomaterials.

[†]Supported by grants from the NIH (to T.P.U.) and the American Heart Association (to N.P.P.). Work in R.R.'s laboratory was supported by start-up funds from Arizona State University.

[*]Address correspondence to this author. Tel: (480) 727-9823. Fax: (480) 727-6183. Tatiana.Ugarova@asu.edu.

Integrins comprise a family of noncovalently associated $\alpha\beta$ heterodimer cell surface receptors that mediate adhesive interactions with the extracellular matrix and other cells. By providing a physical link between the cytoskeleton and the surrounding matrix, integrins regulate a diverse range of processes including growth, differentiation, cell motility, hemostasis, and the immune/inflammatory response. Increasing evidence suggests that integrins participate in these processes by responding and transmitting mechanical stresses across the plasma membrane (1–3). Physical forces sensed by integrins are transduced into intracellular chemical signals which, in turn, result in changes of cell behavior. These forces are developed during cell adhesion when integrins engage their respective ligands in the extracellular matrix. As cells attach, they pull on their surroundings, probing the rigidity of substrates. Therefore, the physical properties of extracellular matrices appear to represent the main signal used by integrins to alter the cellular responses. Indeed, although the molecular pathways are still only partially known, various cells sense and respond distinctly to soft versus rigid substrates (4–6). Adhesion-mediated sensing of substrates with varied rigidity is translated into the differential protein tyrosine phosphorylation and recruitment of signaling molecules to adhesion sites. For example, the sensing of rigidity is involved in remodeling of focal adhesions: cell adhesion to soft substrates results in the formation of diffuse and dynamic adhesion complexes while adhesion to rigid substrates produces stable focal adhesions (7). These observations indicate that signaling functions of ligand–integrin–cytoskeleton complexes are modified depending on the magnitude of forces exerted by rigidity of extracellular matrices. While the relationship between integrins and rigidity responses has been examined in various tissue cells, little is known about how integrins on blood cells respond to adhesive substrates with variable physical properties.

The matrices formed of plasma protein fibrinogen and its clotting product fibrin may represent important biological examples that illustrate how the physical properties of substrates control adhesion of blood cells. Fibrinogen and fibrin are the principal components of thrombi formed at sites of vascular injury. Furthermore, the presence of fibrin(ogen) on implanted vascular grafts is the major factor of their biocompatibility (8). The fibrin(ogen) substrates support attachment of platelets and leukocytes via integrins $\alpha_{IIb}\beta_3$ and $\alpha_M\beta_2$, respectively. Numerous *in vitro* examples have been described in which fibrin and fibrinogen immobilized on plastic (a mimic of fibrin) are highly adhesive for platelets and leukocytes (9, 10). *In vivo*, however, fibrin clots do not support strong cell adhesion (11–14). Adhesive interactions of blood cells with fibrin in the circulation occur in the presence of high concentrations of plasma fibrinogen (~2–4 mg/mL). By virtue of its ability to form complexes with fibrin and its capacity to self-associate, soluble fibrinogen can modify cell adhesion. Therefore, a layer of fibrinogen deposited on the surface of fibrin clots or implanted biomaterials can alter the adhesive properties of these substrates. Indeed, we have recently demonstrated that soluble fibrinogen is a potent inhibitor of integrin-mediated leukocyte adhesion to fibrin and surface-bound fibrinogen and provided evidence that fibrinogen reduces cell adhesion by binding to the fibrin(ogen) substrates (15). Accordingly, cells that engage this “fake” adhesive layer are not able to consolidate their grip when subjected to shear stress; subsequently, cells detach. Conversely, cells that adhere to intact untreated fibrin gel adhere firmly. The mechanisms underlying distinct properties of highly adhesive and antiadhesive fibrin(ogen) surfaces, however, are uncertain.

Taking into consideration the significant role fibrinogen and fibrin play in thrombus formation and thrombogenicity of biomaterials, we have examined the physical properties of fibrin-(ogen) matrices and their ability to support integrin $\alpha_{IIb}\beta_3$-mediated platelet adhesion and outside-in signaling. We show that binding of soluble fibrinogen to the surface of fibrin gel or its deposition at high density on various solid surfaces prevents platelet adhesion. Direct visualization of antiadhesive fibrinogen matrices by atomic force microscopy and analyses of their physical properties by force spectroscopy revealed that fibrinogen deposited at high density forms the multilayered material which is characterized by low adhesion forces. In contrast, immobilization of fibrinogen at low density produces a highly adhesive layer in which single molecules are directly attached to the solid surface and which sustains high rupture forces. In agreement with their distinct physical properties, the single-layer, but not multilayer, fibrinogen substrates induced strong platelet signaling and spreading. The data suggest that platelets sense the physical properties of fibrin(ogen) substrates by adjusting their integrin $\alpha_{IIb}\beta_3$-mediated outside-in signaling which controls overall platelet adhesion and spreading.

MATERIALS AND METHODS

Proteins and Antibodies

Human thrombin and fibrinogen, depleted of fibronectin and plasminogen, were obtained from Enzyme Research Laboratories (South Bend, IN). Fibrinogen was treated with iodoacetamide to inactivate the residual factor XIII. Phenylalanylprolylarginine chlormethyl ketone (PPACK) and polyvinylpyrrolidone (PVP)[1] were from Sigma (St. Louis, MO). Calcein AM was purchased from Molecular Probes (Eugene, OR). mAb AP3 directed against the β_3 integrin subunit was from GTI (Brookfield, WI). Anti-talin mAb (clone 8D4) and normal mouse IgG were from Sigma (St. Louis, MO). The anti-FAK mAb and polyclonal antibody against the integrin β_3 subunit were from Millipore (Billerica, MA). The anti-Syk and anti-phospho-Tyr (PY20) mAbs were from Santa Cruz Biotechnology (Santa Cruz, CA). mAb 2G5 directed against the fibrinogen γC sequence 373–385 and polyclonal anti-skelemin antibody generated against recombinant skelemin fragment were described previously (16, 17). Zysorbin-G was from Invitrogen (Carlsbad, CA), protein A–Sepharose was obtained from Amersham Biosciences Inc. (Piscataway, NJ), and the Immobilon P membrane was purchased from Millipore (Billerica, MA). Alexa Fluor 568 phalloidin was obtained from Invitrogen (Carlsbad, CA). Sodium metavanadate and sodium cacodylate were from Sigma (St. Louis, MO).

Adhesion Assays

Platelets were collected from fresh aspirin-free human blood in the presence of 2.8 μM prostaglandin E_1 and isolated by differential centrifugation followed by gel filtration on Sepharose 2B as described (18). Adhesion assays were performed essentially as described previously (19). Briefly, the wells of 96-well polystyrene microtiter plates (Immulon 4HBX; Thermo-Labsystems, Franklin, MA) were coated with various concentrations of fibrinogen

[1]Abbreviations: AFM, atomic force microscopy; PVP, polyvinylpyrrolidone; PBS, phosphate-buffered saline; HBSS, Hank's balanced salt solution.

for 3 h at 37 °C and postcoated with 1.0% PVP for 1 h at 37 °C. Alternatively, fibrin gels were formed in siliconized Immulon 2 96-well format strips by mixing 100 μL aliquots of 1.5 mg/mL fibrinogen in HBSS with thrombin (0.15 unit/mL) for 2 h at 37 °C. After polymerization, the thrombin activity was quenched by addition of PPACK, and thrombin inactivation was verified with a chromogenic substrate S-2238. Platelets were labeled with 10 μM calcein for 30 min at 37 °C and washed twice with HBSS +0.1% BSA. Aliquots (1×10^7/0.1mL) of labeled platelets were added to each well. For inhibition experiments, the fibrin gels were incubated with different concentrations of soluble fibrinogen for 30 min at 37 °C, after which fibrinogen solutions were aspirated and platelets were added. After 50 min incubation at 37 °C, the nonadherent cells were removed by two washes with PBS. Fluorescence was measured in a CytoFluorII fluorescence plate reader (Applied Biosystems, Foster City, CA).

Immunofluorescence

Glass coverslips were coated with two different concentrations of fibrinogen (2 and 20 μg/mL) for 3 h at 37 °C and blocked with 1% PVP for 1 h at 22 °C. Isolated platelets in Tyrode's solution (3×10^5/mL) were allowed to adhere for 50 min at 37 °C, and nonadherent cells were removed by three washes with PBS. Adherent platelets were fixed for 10 min using 3.7% paraformaldehyde and then incubated with 0.1%Triton X-100 for 5 min to render them permeable. To detect the actin cytoskeleton, permeabilized cells were incubated with Alexa Fluor 568 phalloidin for 20 min at 22 °C followed by three washes with PBS. Samples were mounted with a droplet of Cytoseal 60 mounting medium, and platelets were viewed with a Leica DM4000B immunofluorescence microscope and analyzed by Leica Application Suite, Version 2.5.0.R1 software.

Immunoprecipitation

Platelets were added to the wells of 96-well microtiter plates coated with 2 or 20 μg/mL fibrinogen and allowed to attach for 15, 30, 60, 90, and 120 min at 37 °C. Alternatively, platelets were allowed to adhere to the intact fibrin gel or gels treated with soluble fibrinogen prepared as described above under Adhesion Assays. The nonadherent cells were removed, and adherent platelets were solubilized with a lysis buffer (20 mM Tris-HCl, pH 7.4, 150 mM NaCl, 1% Triton X-100, 1mM$CaCl_2$, 1mMPMSF, 100 μg/mL leupeptin, 10mM benzamidine, and 1 mM sodium metavanadate) for 30 min at 22 °C. Control resting platelets kept in suspension in polysterene tubes were also lyzed with a lysis buffer. After the removal of insoluble material by centrifugation at 12000*g* for 15 min, the lysates were incubated with 10 μg of normal mouse IgG and 50 μL of Zysorbin-G for 2 h at 4 °C. The supernatants were incubated with 1 μg of each mAb AP3 (anti-β_3) or anti-FAK or anti-SYK mAbs for 2 h at 4 °C. The integrin–mAb complexes were then collected by incubating with 50 μL of protein A–Sepharose overnight at 4 °C. The immunoprecipitated proteins were eluted with SDS–PAGE loading buffer, electophoresed on 7.5% SDS-polyacrylamide gels under nonreducing conditions, and analyzed by Western blotting. To detect the presence of selected proteins, Immobilon P membranes were incubated with anti-skelemin polyclonal antibody (1:40000 dilution), anti-β_3 polyclonal antibody (1:4000), anti-talin mAb (1:500), anti-FAK mAb (1:2000), anti-SYK mAb (1:200), and PY20 mAb (1:250) and developed using SuperSignal West Pico substrate (Pierce).

Single Molecule Detection

The amount of fibrinogen bound to the surface of glass coverslips was determined by single molecule fluorescence. Fibrinogen conjugated to Alexa Fluor 647 was purchased from Molecular Probes (Eugene, OR). Different concentrations of fibrinogen in PBS were spiked with fluorescently labeled fibrinogen (1:2000) and adsorbed on coverslips overnight at 4 °C. Images were acquired using an Olympus IX70 inverted microscope equipped with an Olympus UPlanFl 100 × 1.3 NA oil immersion objective. An additional 1.25× magnification was used prior to the camera. The filter cube contained an excitation filter (Semrock FF01-640/14-25), an emission filter (Chroma 690/40), and a dichroic mirror (Chroma z647 rdc). For excitation, a Melles Griot 43 Series ion laser tuned to 647 nm was used. For all experiments, 100 mW of power prior to the microscope objective was used. Images were acquired with a Photometrics Cascade 512B camera using 10 MHz EM Gain 4× adjusted to 4095. Stacks of images were acquired for each field of view. Each frame represents 1 s of integration. For the analysis presented here, five frames were averaged to reduce noise. The number of fluorescently labeled fibrinogen molecules adsorbed on the surface was calculated by the developed algorithm. The algorithm identifies single molecules in a given fluorescence image of a surface.

Atomic Force Microspcopy (AFM) Imaging of Fibrinogen

Different concentrations of fibrinogen (0.02–20 μg/mL) in PBS were deposited on freshly cleaved mica for 3 h at 37 °C. Excess fibrinogen was removed by rinsing the samples with water. The samples were dried with argon gas, and images in air were acquired using an Agilent 5500 scanning probe microscope (Agilent Technologies, Chandler, AZ). Alarge-size scanner which allows measurements on areas up to 100 × 100 μm was used. Imaging was conducted in the amplitude modulation oscillatory mode using Si probes with stiffness in the 1–5 N/m range. The experimental parameters (small free amplitude in the 5–10 nm range and set-point amplitude close to free amplitude) were selected to perform a low-force operation which prevents sample damage. The scan rate was 0.6–1.2 Hz. Image analyses (cross section) were performed using Gwyddion 2.10 software.

The nanolithography procedure was performed to assess the thickness of fibrinogen layers adsorbed at 2, 5, and 20 μg/mL. To remove fibrinogen from the surface, the capability of the Agilent 5500 instrument to operate in the nanolithography mode was utilized. A sample area (2 × 2 μm) was scanned in the contact mode using a stiff probe. In this way, the adsorbed material was pushed away and a “window” formed. A step at the “window” edge which corresponds to the thickness of the fibrinogen layer was then imaged in the oscillatory mode.

Force Spectroscopy

Force–distance measurements were performed in PBS at room temperature using a MFP-3D AFM (Asylum Research, Santa Barbara, CA). Silicon nitride probes (MSCT; Veeco Probes, Camarillo, CA) with nominal spring constants in the range of 15–20 pN/nm were used for force measurements. The spring constants for each cantilever were measured using the MFP-3D’s built in thermal method. The surfaces coated with different concentrations of fibrinogen were probed using a force trigger of 1 nN and approach and retract velocity of 2000 nm/s. Between 1000 and 2000 force distance curves were collected for each surface.

Each curve was analyzed by in-house software written in IGOR Pro 6 (Wavemetrics, Lake Oswego, OR), which calculates adhesion (pull-off) forces. The most probable adhesion forces were obtained from the maximum of the Gaussian fit to the force histogram. In order to examine the effect of fibrinogen, which might potentially adsorb on the tip during the collection of numerous force distance curves, control measurements with tips incubated for 3 h in 20 μg/mL fibrinogen were performed. When probing low- and medium-density fibrinogen surfaces with these modified tips, an initial phase characterized by the lower adhesion force events was observed. However, after this short phase, the system transitioned to a steady state characterized by the same adhesion distributions as when probing with a nonmodified tip. In the typical experiments, the low-density fibrinogen surfaces were measured first. As a control, the low-density fibrinogen surfaces were measured immediately after high-density samples. When measuring in this order, the same force distributions have been observed as when proceeding form low- to high-density substrates.

Scanning Electron Microscopy

Platelet adhesion to the intact fibrin gels or gels coated with soluble fibrinogen was performed as described under Adhesion Assays. Nonadherent platelets were removed by three washes with 0.1 M phosphate buffer (pH 7.4), and fibrin gels with adherent platelets were fixed in 2%glutaraldehyde containing 50 mM sodium cacodylate, pH 7.0, for 30min at 22 °C. The gels were rinsed three timeswith0.1M phosphate buffer (pH 7.4) and incubated with 1% osmium tetroxide in the same buffer for 15 min. After washing, the gels were dehydrated in a graded series of ethanol concentrations over a period of 1.5 h. The clots were critical point dried in liquid CO_2, mounted on aluminum stubs, and then sputter-coated with platinum. The samples were observed in a Leica-Cambridge Stereoscan 360 FE scanning electron microscope (Bannockburn, IL).

RESULTS

Effect of Coating Concentrations of Fibrinogen on Platelet Adhesion

We previously reported that integrin-mediated leukocyte adhesion to immobilized fibrinogen exhibits a characteristic “peak”-like pattern: adhesion is maximal at low coating concentrations of fibrinogen and markedly decreases as the concentration increases (15). To investigate whether platelets exhibit the same behavior, integrin $\alpha_{IIb}\beta_3$-mediated platelet adhesion to various coating concentrations of fibrinogen was examined. Figure 1 shows that platelet adhesion was maximal at a low (~2.5 μg/mL) coating concentration and then declined at higher concentrations. Surfaces coated with 20 μg/mL fibrinogen supported an ~4-fold lower extent of adhesion than those coated with 2.5 μg/mL protein. The $\alpha_{IIb}\beta_3$-mediated adhesion of resting platelets to immobilized fibrinogen is mediated in part by the P3 site in the γC domain of fibrinogen (residues 370–382) (20). This sequence is poorly available in soluble fibrinogen and becomes exposed after immobilization of fibrinogen on various surfaces (16, 21). To examine whether P3 remains exposed in fibrinogen deposited at increasing concentrations, we have used mAb 2G5 which recognizes this sequence. Figure 1 shows that the P3 site was exposed in the range of fibrinogen concentrations (3–50 μg/mL) at which platelet adhesion began to sharply decline. Thus, the decrease in platelet adhesion on the high-density fibrinogen substrates is unlikely due to the masking of the P3

site. Deposition of fibrinogen on other solid materials, including mica and glass, produced a similar “peak”-like pattern of platelet and leukocyte adhesion (not shown). Taken together with previous findings, these results indicate that anomalous cell adhesion to fibrinogen matrices does not depend either on the source of cells or on their integrins and may be controlled by the qualities of fibrinogen substrates.

AFM Study of Fibrinogen Substrates

To characterize the properties of surfaces prepared by deposition of various concentrations of fibrinogen, atomic force microscopy and AFM-based force spectroscopy were used. AFM images of individual fibrinogen adsorbed onmica at 0.02 μg/mL are shown in Figure 2A. The molecules are observed as linear or slightly bent rods with a length of 46.2 ± 2.5 nm and the characteristic globular structure corresponding to the fibrinogen D and E domains (22). At higher concentrations (0.05–0.3 μg/mL), the surfaces are gradually populated with the material, but the molecules are clearly discernible as individual monomers evenly and sparsely attached to mica (Figure 2B, upper row). The images collected after coating mica with 0.6 μg/mL demonstrate that the density of fibrinogen is higher and many molecules lie in close proximity to each other (Figure 2B, middle row). As the coating concentration increases further (0.9–1.2 μg/mL), the surfaces are covered with more material, and individual molecules are poorly discriminable. At still higher concentration (1.5 μg/mL), the fibrinogen layer becomes denser, and the surface appears as though the molecules begin to pile up (Figure 2B, bottom row). Coating mica at ≥2 μg/mL results in the formation of a thicker coat formed of multiple layers of aggregating fibrinogen. As measured by the nanolithography procedure, the thickness of a layer produced by deposition of 2.0 μg/mL fibrinogen was ~2.0 ± 0.9 nm (Figure 2C, D). The depth of protein layers produced by immobilization of fibrinogen at 5 and 20 μg/mL was 4.7 ± 0.9 and 8.8 ± 1.1 nm, respectively. Thus, the changes in the surface features following the gradual increase in the coating concentrations of fibrinogen show that the molecules deposited at low concentrations (0.02–0.9 μg/mL) make direct contact with the solid surface. In contrast, molecules deposited at higher concentrations not only are attached to the mica but also interact with each other forming a multilayer material. These data provide direct visualization of fibrinogen adsorption at different coating concentrations and allow a correlation of the pattern of deposition with cell adhesion.

To characterize the fibrinogen surfaces further, AFM-based force spectroscopy was used (23). Different concentrations of fibrinogen were immobilized on mica and glass, and the surfaces were probed with silicon nitride AFM tips. The adhesion force was measured by calculating the force difference between the pull-off point and the baseline. Between 1000 and 2000 distance curves for each surface were collected. Panels A and B of Figure 3 show a representative force curve and the histograms of distribution of adhesion forces for selected concentrations (0.6 and 1.2 μg/mL) of fibrinogen on mica, respectively. Figure 3C shows the most probable adhesion forces obtained from the Gaussian fits to the histograms versus the fibrinogen coating concentrations on mica (left panel) and glass (right panel). The results demonstrate that the surface–AFM tip interaction is the strongest at ~0.7–0.9 μg/mL coating concentrations of fibrinogen adsorbed on both surfaces. The adhesion declines sharply as the coating concentration increases up to 1.2 μg/mL and remains low at 2 μg/mL

and higher (not shown). The reason for the higher adhesion forces obtained for fibrinogen adsorbed on glass compared to mica is not clear and may tentatively be attributed to different properties of solid materials themselves, such as their roughness and/or rigidity. Nevertheless, the difference in adhesion forces between the highly adhesive and low adhesive fibrinogen substrates adsorbed on these materials is very similar (~3- and 3.5-fold for mica and glass, respectively). When correlated with AFM images, the data indicate that adhesion forces are the highest when fibrinogen molecules are directly attached to the surface (0.7–0.9 μg/mL). Moreover, when fibrinogen density increases and the molecules self-associate to form a thick layer of material, there is a decline in the adhesion force. Thus, surfaces formed at low and high coating densities of fibrinogen differ in their topographical and adhesive properties. Most remarkable is the fact that the dependence of the most probable adhesion forces on various fibrinogen substrates closely recapitulates the “peak”-like pattern of cell adhesion.

Platelet Spreading on Different Fibrinogen Substrates

It is well-known that ligand engagement by integrins induces outside-in signaling manifesting in the recruitment of cytoplasmic molecules to the integrin cytoplasmic tails and in the cytoskeleton reorganization resulting in cell spreading. The difference in cell adhesion to fibrinogen coated at low and high densities suggests that these substrates may initiate differential outside-in signaling. To investigate this possibility, we initially examined platelet spreading on glass coverslips coated with two fibrinogen concentrations (2 and 20 μg/mL) as representative highly and poorly adhesive substrates, respectively. The number of platelets adherent to fibrinogen adsorbed at low density was ~2.5-fold higher than that on high-density fibrinogen. This difference was not due to the abnormal adsorptive capacity of glass. Using single molecule detection, we verified that deposition of fibrinogen on glass obeys a normal adsorption isotherm (Figure 4A). To determine cell spreading, platelets were allowed to adhere on fibrinogen-coated coverslips for 50 min at 37 °C. Cells were then fixed and stained with phalloidin, and actin stress fibers were visualized by immunofluorescence. As shown in Figure 4B, platelets adherent on a low-density fibrinogen were fully spread (upper panel), while those on a high-density fibrinogen remained round (bottom panel). Taken together, these observations indicate that platelet adhesion to fibrinogen surfaces displaying different physical properties induces differential platelet spreading.

Differential Recruitment of Skelemin and Talin to the $\alpha_{IIb}\beta_3$ Cytoplasmic Tails during Platelet Adhesion to Fibrinogen Immobilized at Low and High Densities

To investigate the possibility that differential cell spreading on various fibrinogen substrates results from differences in outside-in signaling, we examined recruitment of cytoplasmic molecules to $\alpha_{IIb}\beta_3$. We recently reported that platelet adhesion to immobilized fibrinogen induces unclasping of the cytoplasmic tails of integrin $\alpha_{IIb}\beta_3$ enabling binding of the cytoplasmic protein skelemin (17). Therefore, skelemin was used as a probe of the initial outside-in signaling in platelets adherent to different fibrinogen substrates. Platelets were allowed to adhere to microtiter wells coated with 2 and 20 μg/mL fibrinogen, and the amount of skelemin recruited to $\alpha_{IIb}\beta_3$ was determined by immunoprecipitation analyses using anti-β_3 mAb AP3 followed by Western blotting with anti-skelemin antibodies. As shown in Figure 5A (middle panel) and assessed by densitometry analyses (Figure 5B),

platelet adhesion to fibrinogen coated at 2 μg/mL resulted in ~4-fold higher levels of skelemin associated with $\alpha_{IIb}\beta_3$ compared to that on high-density fibrinogen.

Another cytoskeletal protein that interacts with the membrane-proximal α_{IIb} and β_3 cytoplasmic segments involved in the clasp is talin (24). Therefore, the recruitment of talin to $\alpha_{IIb}\beta_3$ during cell adhesion to different fibrinogen substrates was examined. In the initial experiments, we demonstrated that talin does not associate with $\alpha_{IIb}\beta_3$ in resting platelets in suspension (Figure 5C; see a lane marked "0" in which talin is clearly absent in the complex with the integrin β_3 subunit) and is recruited to the integrin after the initiation of cell adhesion (Figure 5C, lanes 2–6). These data indicate that, similar to skelemin, talin interacts with the membrane-proximal segments of the α_{IIb} and β_3 tails only after the initiation of adhesion. Association of talin with $\alpha_{IIb}\beta_3$ in platelets adherent to surfaces coated with 2 and 20 μg/mL fibrinogen was then compared. The amount of talin in complex with $\alpha_{IIb}\beta_3$ isolated from platelets adherent to low-density fibrinogen was ~5-fold higher than that on high-density fibrinogen (Figure 5A, bottom panel, and Figure 5B). Thus, platelet adhesion to substrates formed by adsorption of low concentrations of fibrinogen results in significantly higher levels of skelemin and talin recruited to the α_{IIb} and β_3 cytoplasmic tails than adhesion to high-density fibrinogen.

Induction of Tyrosine Kinase Phosporylation during Platelet Adhesion to Different Fibrinogen Substrates

To further investigate the relationship of outside-in signaling in platelets and the properties of fibrinogen substrates, we examined phosphorylation of two tyrosine kinases, FAK and Syk. Both tyrosine kinases have been implicated in integrin outside-in signaling in platelets. Platelets were allowed to adhere for 50 min at 37 °C to dishes coated with 2 and 20 μg/mL fibrinogen. Nonadherent cells were removed, adherent platelets were lysed, and FAK was immunoprecipitated with anti-FAK specific monoclonal antibody. FAK phosphorylation was detected on Western blots using anti-phosphotyrosine mAb PY20. After normalizing for a total FAK protein in the immunoprecipitated material, the amount of phosphorylated FAK was determined by densitometry scanning. As shown in Figure 6A, platelet adhesion to 2 μg/mL fibrinogen resulted in an ~3-fold increase in the amount of phosphorylated FAK compared to that on 20 μg/mL fibrinogen. We sought to verify that differential FAK phosphorylation observed after 50 min adhesion on two fibrinogen substrates was not due to differences in the kinetics of protein phosphorylation. FAK was immunoprecipitated 30, 45, and 60min after adhesion on surfaces coated with 2 and 20 μg/mL fibrinogen, and the amount of phosphorylated FAK was assessed after adjusting for a total FAK protein. FAK phosphorylation gradually increased on both substrates, and at each time point the amount of phosphorylated FAK was higher in platelets adherent to low-density fibrinogen than that on high density (not shown). In additional studies, phosphorylation of Syk was determined. Platelet lysates obtained after 50 min adhesion on low- and high-density fibrinogen substrates were immunoprecipitated with anti-Syk mAb, and the levels of phospho-Syk were determined using mAb PY20. As shown in Figure 6B, ~3-fold higher levels of Syk were phosphorylated in platelets adherent to 2 μg/mL fibrinogen than in those to 20 μg/mL fibrinogen. Thus, these results suggest that platelets sense different fibrinogen substrates by responding with differential phosphorylation of signaling molecules FAK and Syk.

Binding of Soluble Fibrinogen to Fibrin Clot Inhibits Platelet Adhesion

To explore a model which is more representative of physiological conditions, we examined whether soluble fibrinogen protects fibrin gels from platelet attachment. The fibrin gels were overlaid with solutions containing different concentrations of fibrinogen for 30 min at 37 °C, solutions above the gels were aspirated, and platelet adhesion was determined. As shown in Figure 7A, treatment of fibrin gels with fibrinogen inhibited platelet adhesion. At 500 μg/mL, added fibrinogen blocked adhesion by ~75% compared to nontreated gels.

Next, to examine platelet spreading, platelets were allowed to adhere to either intact fibrin gel or gels coated with 1.0 mg/mL soluble fibrinogen. Cells were then fixed and examined using scanning electron microscopy. As shown in Figure 7B (upper panel), platelets adherent to intact fibrin gel were fully spread and exhibited numerous extended pseudopods protruding from the cell's body. The morphology of platelets adherent to the gel coated with fibrinogen was markedly different and revealed cells that remained largely round, suggesting a low extent of their activation (Figure 7B, bottom panel).

Experiments were then performed to determine whether different levels of skelemin and talin associated with $\alpha_{IIb}\beta_3$ in platelets adherent to the intact fibrin gel or fibrin coated with fibrinogen. Figure 8A schematically depicts the surfaces to which platelets adhere. As shown in Figure 8B, C, significantly higher levels of skelemin and talin were detected in immune complexes obtained from platelets adherent to the intact fibrin gel as compared to those adherent to the layer of fibrinogen on the surface of fibrin (~7- and 5-fold, respectively). In additional experiments, intact fibrin gels and fibrin coated with fibrinogen were used to obtain evidence for differential FAK and Syk phosphorylation. As shown in Figure 8D, significantly higher levels of phosphorylated FAK (~5-fold) were detected in platelets adherent to untreated fibrin than to fibrin gels pretreated with fibrinogen. Likewise, platelet adhesion to untreated fibrin resulted in an ~2-fold increase in phosphorylation of Syk compared to adhesion on fibrin covered with fibrinogen (Figure 8E). Taken together, these observations suggest that binding of soluble fibrinogen to fibrin renders the surface of the gel nonadhesive for platelets as a result of diminished cellular signaling.

DISCUSSION

In a previous study we demonstrated that binding of soluble fibrinogen to fibrin gels or its immobilization at high density renders the substrates nonadhesive for leukocytes (15). The present study extends these findings to platelets. We show that deposition of fibrinogen on various surfaces, including fibrin clots, reduces platelet adhesion. In conjunction with our previous report, the results presented here support the model that fibrinogen exerts its antiadhesive effect by modifying the substrates. Accordingly, deposition of fibrinogen as a multilayered material changes the physical properties of surfaces, transforming them into substrates with reduced adhesiveness. These alterations result in the reduced ability of platelet integrin $\alpha_{IIb}\beta_3$ to induce outside-in signaling, manifested in diminished tyrosine kinase phosphorylation and decreased recruitment of cytoplasmic proteins skelemin and talin to the α_{IIb} and β_3 cytoplasmic tails. Thus, the net result is the inability of surfaces formed of self-assembled fibrinogen to support firm cell adhesion and spreading. We

suggest that binding of fibrinogen to fibrin clots or its deposition on the surface of biomaterials may play significant roles in control of adhesion and signaling of blood cells.

Fibrinogen deposited on solid surfaces at high density did not support firm platelet adhesion whereas at low density it was highly adhesive (Figure 1). A similar abnormal pattern of adhesion was observed earlier with leukocytes (15). Based upon the analyses of a “peak of adhesion”, we have previously proposed that fibrinogen adsorbed at low density makes direct contact with the plastic surface and, therefore, binds firmly. In contrast, fibrinogen adsorbed at higher densities would not only bind to plastic but also form bonds with other fibrinogen molecules. Direct visualization of fibrinogen deposition using AFM imaging confirmed this proposal (Figure 2). The images of fibrinogen immobilized at low coating concentrations revealed individual molecules attached directly to mica. In contrast, adsorption of fibrinogen at high coating concentrations (>2 μg/mL) led to a high-level protein coverage and produced a thick layer of material (Figure 2B). Probing adhesive properties of these surfaces by force spectroscopy demonstrated that they are characterized by distinct adhesion forces, with the highest forces produced by a lower density fibrinogen. These data provide support for the idea that different adhesion forces generated by the low- and high-density fibrinogen substrates may be responsible for different cell adhesion.

Distinct physical properties of low- and high-density fibrinogen substrates closely correlated with their cell adhesive properties; i.e., low-density fibrinogen is highly adhesive while a multilayer substrate is not able to support firm adhesion. The greater cell adhesion on low-density fibrinogen appears to arise as response to the resistance derived from the solid surface to which fibrinogen molecules are attached firmly. Hence, the substrate may not yield when cellular integrins pull on it. Conversely, material formed by deposition of high concentrations of fibrinogen, either directly on solid surfaces or as a coat on the surface of fibrin gels, may support low adhesion because this multilayered matrix cannot resist the cytoskeleton pulling and is likely to transmit low forces. At present, the molecular basis for the antiadhesive properties of high-density fibrinogen substrates is unclear, and further experiments are needed to address the relationships between mechanical and structural properties of various fibrinogen substrates and cell adhesion.

It appears that platelets sense and respond to the resistance of fibrin(ogen) substrates by adjusting their adhesion through modulating the recruitment of cytoskeletal molecules, tyrosine kinase phosphorylation, and the state of their cytoskeleton. Previous studies identified several cytoplasmic molecules which interact with the cytoplasmic tails of $\alpha_{IIb}\beta_3$. Among them, skelemin is essential for the formation of initial integrin clusters and integrin-induced cell spreading (25). Another protein, talin, connects integrin cytoplasmic tails with actin cytoskeleton and participates in force sensing during adhesion (26, 27). We have recently demonstrated that the binding sites for skelemin in the membrane-proximal parts of α_{IIb} and β_3 cytoplasmic tails are cryptic and that the unclasping of tails during platelet adhesion results in their unmasking (17). The finding that talin does not associate with $\alpha_{IIb}\beta_3$ in resting platelets suggests that its binding site in the membrane-proximal segments of the $\alpha_{IIb}\beta_3$ cytoplasmic domain may also be hidden. The results further indicate that engagement of the fibrin(ogen) matrices initiates the conformational change in the cytoplasmic domain of $\alpha_{IIb}\beta_3$ resulting in talin binding. Platelet adhesion to low-density fibrinogen as well as to

intact fibrin was accompanied by a severalfold higher recruitment of skelemin and talin to the cytoplasmic domain of $\alpha_{IIb}\beta_3$ than adhesion to high-density fibrinogen or to fibrinogen bound to fibrin. Differential association of skelemin and talin with $\alpha_{IIb}\beta_3$ suggests that highly adhesive low-density fibrinogen substrate initiates the conformational change of a larger scale.

Growing evidence indicates that tyrosine kinases and phosphatases are directly involved in the force sensing mechanism (5, 28). Consistent with the role of signaling in sensing the physical properties of substrates, tyrosine phosphorylation of two selected kinases, FAK and Syk, was severalfold higher in platelets adhered to fibrinogen immobilized at low density and intact fibrin gels when compared to cells attached to high-density fibrinogen and fibrinogen-coated fibrin. Previous studies on epithelial cells and fibroblasts which exploited inert polyacrylamide gels with a thin coating of covalently attached collagen demonstrated that FAK was involved in sensing rigidity of gels (7, 29). The data presented here show that FAK phosphorylation is also involved in platelet responses to fibrinogen substrates showing different adhesion forces. In addition, the extent of Syk phosphorylation is regulated by the physical properties of fibrin(ogen) substrates with more adhesive substrates eliciting stronger phosphorylation. Correlations have long been made between integrin outside-in signaling, including FAK activation, and increased cell spreading which, at the subcellular level, involves the actin cytoskeleton. The finding that platelets do not spread on fibrin(ogen) surfaces that exhibit low adhesion forces suggests that these substrates limit the ability of platelets to spread by failing to induce sufficient signaling. The molecular pathways of force sensing in platelets remain unknown, and additional studies will be needed to identify the components of the force-sensing machinery assembled at the fibrinogen–$\alpha_{IIb}\beta_3$-cytoskeletal linkages.

The finding of the present work is consistent with previous studies by Jirouskova et al. (30). Using two concentrations (3 and 100 μg/mL) of immobilized fibrinogen, these authors demonstrated differential $\alpha_{IIb}\beta_3$-mediated signaling in platelets. However, their interpretation of this effect was different, i.e., that fibrinogen molecules are oriented vertically on the surface when immobilized at high density and horizontally at low density. Consequently, deposition of fibrinogen at low density results in exposure of new integrin binding sites contributing to the unique outside-in signaling whereas different integrin binding sites are exposed in fibrinogen oriented vertically. This proposal is based mainly on the differential reactivity of antibodies with fibrinogen immobilized at different densities (31). Our data demonstrated that at low density fibrinogen molecules were indeed deposited in the horizontal orientation. However, its immobilization at higher density (1.5–20 μg/mL) resulted in the formation of a multilayered material rather than a single layer of vertically oriented molecules. Although we cannot exclude the possibility that some molecules are packed in the vertical orientation, the majority of them seem to aggregate in a random orientation. Furthermore, our data indicated that exposure of P3, the binding site for $\alpha_{IIb}\beta_3$ in the γC domain of fibrinogen (19, 20), is not altered in the high-density fibrinogen substrates. On the basis of our analyses of adsorption of ^{125}I-labeled fibrinogen (15), we have calculated that 1.7×10^{11} molecules can be adsorbed on the surface of a microtiter well at 2.5 μg/mL (a concentration that produces maximal cell adhesion). Assuming that one

fibrinogen molecule occupies either 230 or 25 nm^2 in the horizontal and vertical orientation, respectively, 1.3×10^{11} and 1.2×10^{12} molecules can bind per a well. Of the two numbers, the former is in close agreement with that found experimentally. Thus, the simplest interpretation of differential cell signaling, which is also supported by examples from other mechanosensitive integrin systems, is that $\alpha_{IIb}\beta_3$ may transduce different physical forces when platelets adhere to low- and high-density fibrinogen substrates. Further studies may help to define the contribution of different mechanisms to platelet adhesion on various fibrin(ogen) matrices.

The relationship between the physical properties of substrates and adhesion similar to that presented in this study has been found using various synthetic materials, including ECM-coated polyacrylamide gels, layer-by-layer polymer assemblies, and microfabricated pillars (7, 32, 33, 28, 34). In contrast with these artificial surfaces, the system described in this study recapitulates the characteristics of natural fibrin(ogen) matrices produced *in vivo*. In the circulation, which has a high concentration of fibrinogen, the surface of fibrin clots is likely to have a coat of fibrinogen (35). Therefore, this matrix may control adhesion of blood cells by mediating different signaling responses. In this regard, numerous previous studies documented that the lumenal surface of blood clots formed in response to vessel injury rapidly becomes nonadhesive to further platelet accumulation (36, 12, 37). Since fibrin and fibrinogen continue to accumulate long after the recruitment of platelets ceases, it is tempting to speculate that the antiadhesive fibrinogen shell may limit thrombus growth under flow conditions. It is likely that the same natural antiadhesive mechanism consisting of the “fibrinogen shield” might protect fibrin clots from excessive leukocyte recruitment. Therefore, a continual feedback between platelet and leukocyte sensing of the physical properties of fibrin(ogen) matrices and their adhesion may regulate thrombus growth and its dissolution in normal hemostasis. Furthermore, the physical properties of fibrin(ogen) matrices can change in disease, thereby altering cellular signaling and adhesion.

Acknowledgments

We acknowledge the Nanoimaging Core Facility at the University of Nebraska Medical Center for generating preliminary AFM and force spectroscopy data. We thank Luda Shlyakhtenko and Alexander Lushnikov for help in conducting the initial AFM experiments.

References

1. Geiger B, Bershadsky A. Exploring the neighbourhood: adhesion-coupled cell mechanosensors. Cell. 2002; 110:139–142. [PubMed: 12150922]
2. Bershadsky AD, Balaban VQ, Geiger B. Adhesion-dependent cell mechanosensitivity. Annu Rev Cell Dev Biol. 2003; 19:677–695. [PubMed: 14570586]
3. Katsumi A, Orr AW, Tzima E, Schwartz A. Integrins in mechanotransduction. J Biol Chem. 2004; 279:12001–12004. [PubMed: 14960578]
4. Discher DE, Janmey P, Wang YL. Tissue cells feel and respond to the stiffness of their substrate. Science. 2005; 310:1139–1143. [PubMed: 16293750]
5. Giannone G, Sheetz MP. Substrate rigidity and force define form through tyrosine phosphatase and kinase pathways. Trends Cell Biol. 2006; 16:213–223. [PubMed: 16529933]
6. Vogel V, Sheetz M. Local force and geometry sensing regulate cell functions. Nat Rev. 2006; 7:265–275.

7. Pelham RJ, Wang YL. Cell locomotion and focal adhesions are regulated by substrate flexibility. Proc Natl Acad Sci USA. 1997; 94:13661–13665. [PubMed: 9391082]
8. Hasegawa T, Okada K, Takano Y, Hiraishi Y, Okita Y. Autologous fibrin-coated small-caliber vascular prostheses improve antithombogenicity by reducing immunological response. J Thorac Cardiovasc Surg. 2007; 135:1268–1276. [PubMed: 17467440]
9. Ruggeri ZM, Mendolicchio GL. Adhesion mechanisms in platelet function. Circ Res. 2007; 100:1673–1685. [PubMed: 17585075]
10. Kuijper PHM, Torres HIG, van der Linden JAM, Lammers JWJ, Sixma JJ, Zwaginga JJ, Koenderman L. Neutrophil adhesion to fibrinogen and fibrin under flow conditions is diminished by activation and L-selectin shedding. Blood. 1997; 89:2131–2138. [PubMed: 9058736]
11. Groves HM, Kinlough-Rathbone RL, Richardson M, Jorgensen L, Moore S. Thrombin generation and fibrin formation following injury to rabbit neointima. Lab Invest. 1982; 46:605–612. [PubMed: 7087391]
12. van Ryn J, Lorenz M, Merk H, Buchanan M, Eisert WG. Accumulation of radiolabeled platelets and fibrin on the carotid artery of rabbits after angioplasty: effects of heparin and dipyridamole. Thromb Haemostasis. 2003; 90:1179–1186. [PubMed: 14652654]
13. van Aken PJ, Emeis JJ. Organization of experimentally induced arterial thrombosis in rats: the first six days. Artery. 1982; 11:156–173. [PubMed: 7171326]
14. McGuiness CL, Humphries J, Waltham M, Burnand KG, Collins M, Smith A. Recruitment of labelled monocytes by experimental venous thrombi. Thromb Haemostasis. 2001; 85:1018–1024. [PubMed: 11434678]
15. Lishko VK, Burke T, Ugarova TP. Anti-adhesive effect of fibrinogen: a safeguard for thrombus stability. Blood. 2007; 109:1541–1549. [PubMed: 16849640]
16. Zamarron C, Ginsberg MH, Plow EF. Monoclonal antibodies specific for a conformationally altered state of fibrinogen. Thromb Haemostasis. 1990; 64:41–46. [PubMed: 1703332]
17. Podolnikova NP, O'Toole TE, Haas TA, Lam SCT, Fox JEB, Ugarova TP. Adhesion-induced unclasping of cytoplasmic tails of integrin $\alpha_{IIb}\beta_3$. Biochemistry. 2009; 48:617–629. [PubMed: 19117493]
18. Ugarova TP, Budzynski AZ, Shattil SJ, Ruggeri ZM, Ginsberg MH, Plow EF. Conformational changes in fibrinogen elicited by its interaction with platelet membrane glycoprotein GPIIb-IIIa. J Biol Chem. 1993; 268:21080–21087. [PubMed: 7691805]
19. Podolnikova NP, Gorkun OV, Loreth RM, Lord ST, Yee VC, Ugarova TP. A cluster of basic amino acid residues in the γ370–381 sequence of fibrinogen comprises a binding site for platelet integrin $\alpha_{IIb}\beta_3$ (GPIIb/IIIa). Biochemistry. 2005; 44:16920–16930. [PubMed: 16363805]
20. Podolnikova NP, Yakubenko VP, Volkov GL, Plow EF, Ugarova TP. Identification of a novel binding site for platelet integrins $\alpha_{IIb}\beta_3$(GPIIbIIIa) and $\alpha_5\beta_1$ in the γC-domain of fibrinogen. J Biol Chem. 2003; 278:32251–32258. [PubMed: 12799374]
21. Zamarron C, Ginsberg MH, Plow EF. A receptor-induced binding site in fibrinogen elicited by its interaction with platelet membrane glycoprotein IIb-IIIa. J Biol Chem. 1991; 266:16193–16199. [PubMed: 1714910]
22. Sit SP, Marchant RE. Surface-dependent conformation of human fibrinogen observed by atomic force microscopy under aqueous conditions. Thromb Haemostasis. 1999; 82:1053–1060. [PubMed: 10494763]
23. Butt HJ, Cappella B, Kappl M. Force measurements with the atomic force microscope: technique, interpretation and applications. Surf Sci Rep. 2005; 59:1–152.
24. Patil S, Jedsadayanmata A, Wencel-Drake JD, Wang W, Knezevic I, Lam SCT. Identification of a talin-binidng site in the integrin beta3 subunit distinct from the NPLY regulatory motif of post-ligand binding functions. The talin N-terminal head domain interacts with the membrane-proximal region of the beta3 cytoplasmic tail. J Biol Chem. 1999; 274:28575–28583. [PubMed: 10497223]
25. Reddy KB, Bialkowska K, Fox JEB. Dynamic modulation of cytoskeletal proteins linking integrins to signaling complexes in spreading cells. J Biol Chem. 2001; 276:28300–28308. [PubMed: 11382766]

26. Giannone G, Jiang G, Suttin DH, Critchley DR, Sheikh S. Talin 1 is critical for force-dependent reinforcement of initial integrin-cytoskeleton bonds but not tyrosine kinase activation. J Cell Biol. 2003; 163:409–419. [PubMed: 14581461]
27. Zhang X, Jiang G, Cai Y, Monkley SJ, Critchley DR, Sheetz MP. Talin depletion reveals independence of initial cell spreading from integrin activation and traction. Nat Cell Biol. 2008; 10:1062–1068. [PubMed: 19160486]
28. Geiger B, Spatz JP, Bershadsky AD. Environmental sensing through focal adhesions. Nat Rev. 2009; 10:21–33.
29. Wang HB, Dembo M, Hanks SK, Wang YL. Focal adhesion kinase is involved in mechanosensing during fibroblast migration. Proc Natl Acad Sci USA. 2001; 98:11295–11300. [PubMed: 11572981]
30. Jirouskova M, Jaisawal JK, Coller BS. Ligand density dramatically affects integrin αIIb*β*3-mediated platelet signaling and spreading. Blood. 2007; 109:5260–5269. [PubMed: 17332246]
31. Moskowitz KA, Kudryk B, Coller BS. Fibrinogen coating density affects the conformation of immobilized fibrinogen: implications for platelet adhesion and spreading. Thromb Haemostasis. 1998; 79:824–831. [PubMed: 9569199]
32. Georges PC, Janmey PA. Cell type-specific response to growth on soft materials. J Appl Physiol. 2005; 98:1547–1553. [PubMed: 15772065]
33. Richert L, Engler AJ, Discher DE, Picart C. Elasticity of native and cross-linked polyelectrolyte multilayer films. Biomacromolecules. 2004; 5:1908–1916. [PubMed: 15360305]
34. Engler A, Bacakova L, Newman C, Hategan A, Griffin M, Discher DE. Substrate compliance versus ligand density in cell on gel responses. Biophys J. 2004; 86:617–628. [PubMed: 14695306]
35. Mizuno T, Sugimoto M, Matsui H, Hamada M, Shida Y, Yoshioka A. Visual evaluation of blood coagulation during mural thrombogenesis under high shear blood flow. Thromb Res. 2008; 121:855–864. [PubMed: 17900667]
36. Baumgartner HR. The role of blood flow in platelet adhesion, fibrin deposition, and formation of mural thrombi. Microvasc Res. 1973; 5:167–179. [PubMed: 4694283]
37. Sim DS, Flaumenhaft R, Furie BC, Furie B. Interactions of platelets, blood-borne tissue factor, and fibrin during arteriolar thrombus formation in vivo. Microcirculation. 2005; 12:301–311. [PubMed: 15814438]

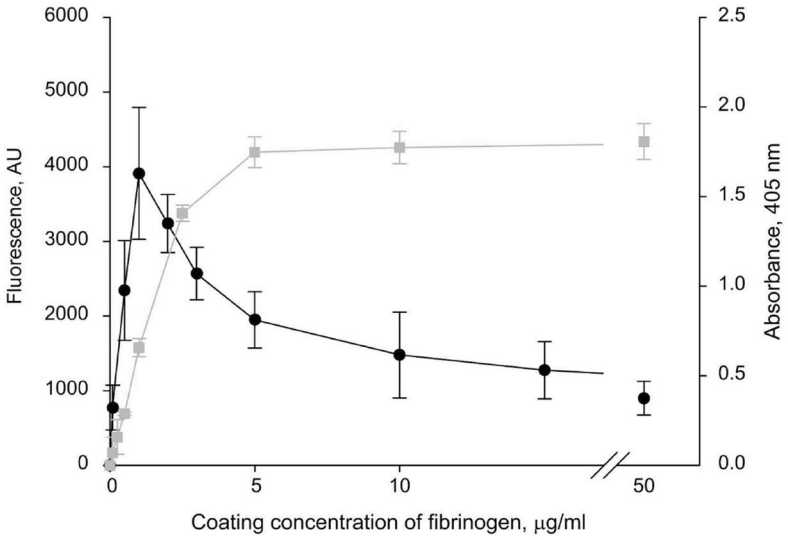

Figure 1.

Platelet adhesion to immobilized fibrinogen. Left ordinate: The wells of 96-well microtiter plates were coated with different concentrations of fibrinogen (0.1–50 μg/mL) for 3 h at 37 °C followed by postcoating with 1%PVP. Aliquots (100 μL) of labeled platelets (1×10^8/mL) were added to each well. After 50 min incubation at 37 °C, the nonadherent cells were removed by two washes with PBS, and fluorescence was measured. Adhesion is shown as fluorescence in arbitrary units. The data shown are the means ± SE of four experiments with triplicate determinations at each experimental point. Maximal platelet adhesion was 17.3 ± 3.5% of added cells. Right ordinate: The wells of microtiter plates were coated with different concentrations of fibrinogen as described above, and mAb 2G5 was added at 1 μg/mL. After incubation for 1 h at 37 °C, the microtiter plates were washed, and goat anti-mouse IgG conjugated to alkaline phosphatase was added. The binding was detected by reaction with *p*-nitrophenyl phosphate, measuring the absorbance at 405 nm.

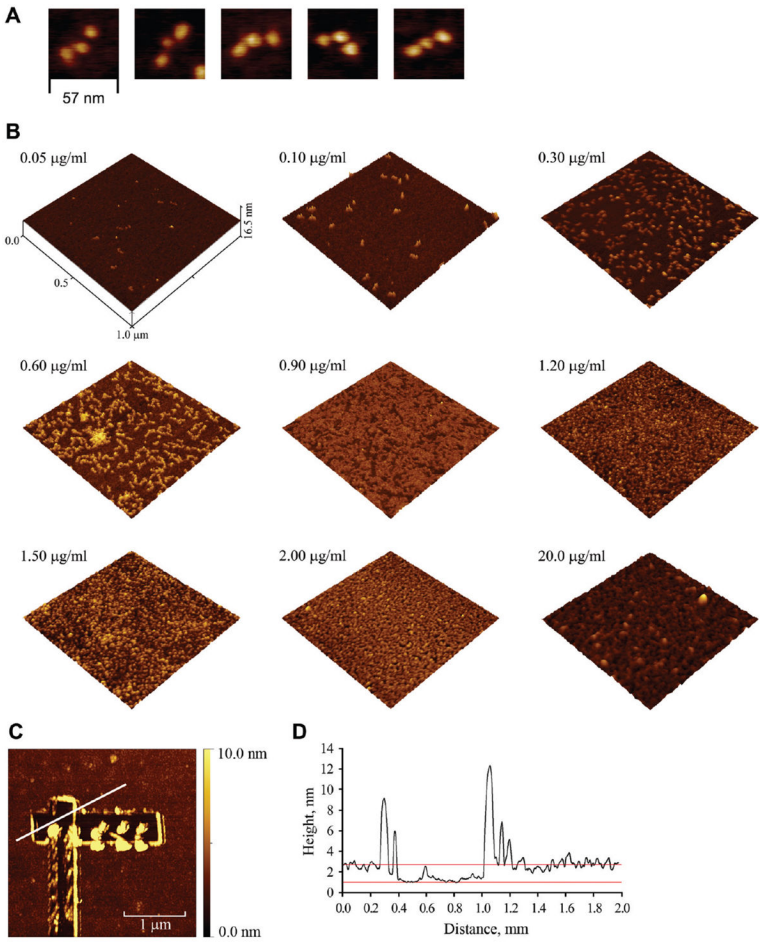

Figure 2.

AFM images of fibrinogen deposited at different coating concentrations on mica. Freshly cleaved mica was coated with different concentrations of fibrinogen for 3 h at 37 °C, and excess fibrinogen was removed by rinsing the samples with water. (A)Height images of individual fibrinogen molecules deposited at 0.02 μg/mL. Five representative molecules are shown. (B) Height images of fibrinogen deposited on mica at selected concentrations (0.05, 0.1, 0.3, 0.6, 0.9, 1.2, 1.5, 2.0, and 20 μg/mL). (C) The layer produced by adsorption of 2 μg/mL fibrinogen was removed from the surface by nanolithography as described in Materials and Methods. (D) The depth of the layer prepared by deposition of 2 μg/mL fibrinogen (shown in (C)) was measured from the plot of the cross section of the surface.

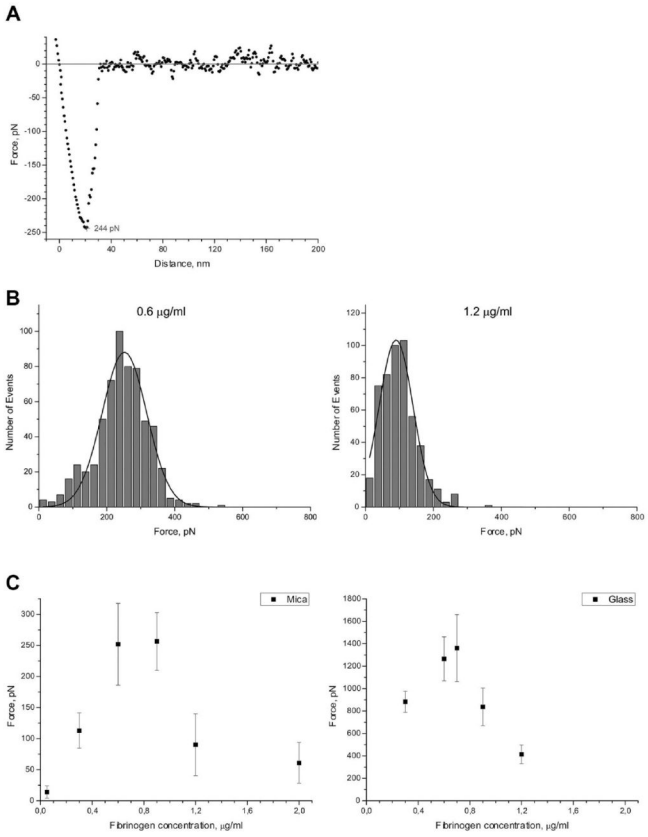

Figure 3.

Force spectroscopy analyses of fibrinogen deposited at various concentrations. (A)Retracting part of a representative force–distance curve obtained on mica coated with 0.6 *μ*g/mL fibrinogen with a retract velocity of 2000 nm/s. The adhesion force is 244 pN. (B) Representative histograms with Gaussian fits of adhesion forces for selected (0.6 and 1.2 *μ*g/mL) concentrations of fibrinogen deposited on mica under conditions described in Figure 2. (C) The most probable adhesion forces plotted as a function of fibrinogen coating concentration adsorbed on mica (left panel) and glass (right panel).

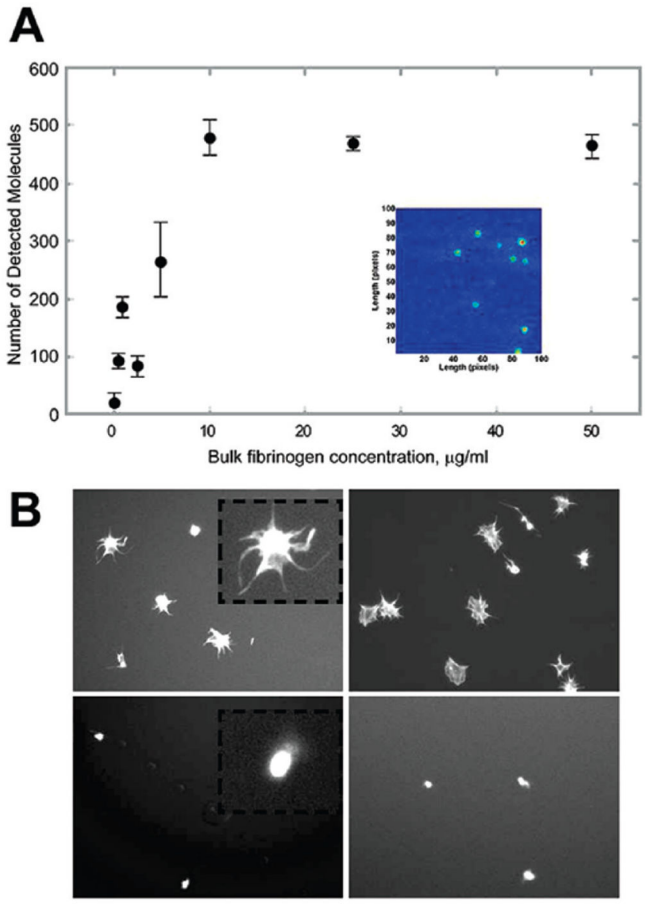

Figure 4.

Morphology of platelets spread on various fibrinogen surfaces. (A) Adsorption of fibrinogen on glass coverslips was assessed by single molecule detection. Glass coverslips were coated with different concentrations of fibrinogen spiked with Alexa Fluor 647-conjugated fibrinogen (dilution 1:2000) for 3 h at 37 °C and rinsed with PBS, and the number of adsorbed fluorescent molecules was detected as described in Materials and Methods. Inset: A representative image of fluorescent fibrinogen molecules is shown. (B) Glass coverslips were coated with 2 μg/mL (upper panel) and 20 μg/mL (bottom panel) fibrinogen and postcoated with 1% PVP. Platelets were allowed to adhere and spread for 50 min at 37 °C. The cells were fixed, permeabilized, and stained with rhodomine–phalloidin for F-actin. Two representative fields of platelets spread on fibrinogen immobilized at two different coating concentrations are shown (magnification 40×). Insets: Enlarged images of representative cells are shown.

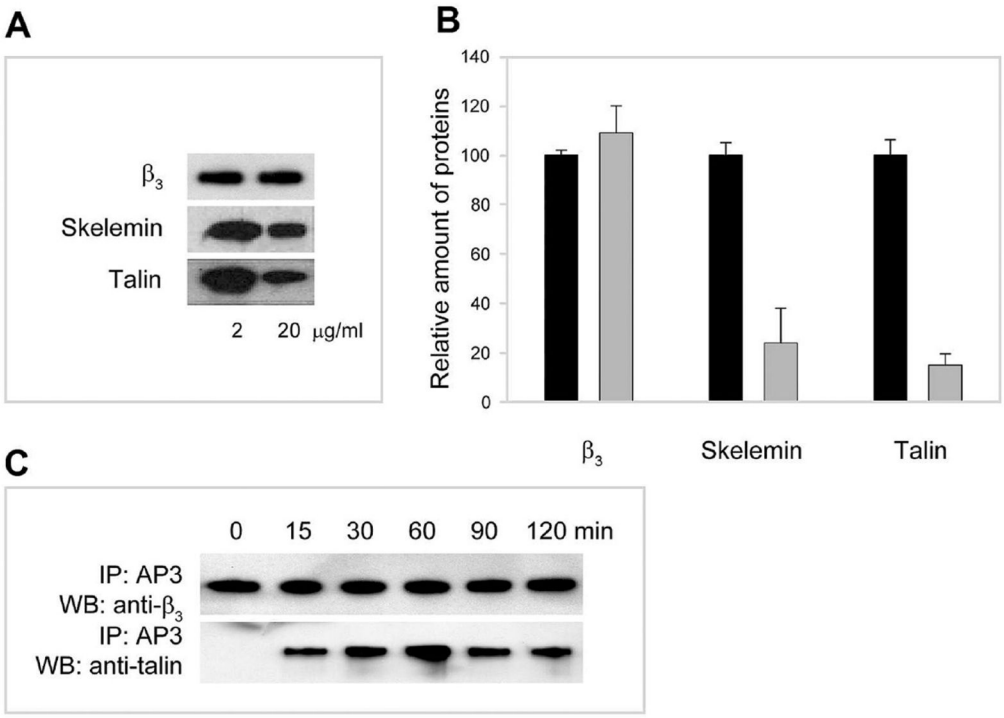

Figure 5.

Differential association of skelemin and talin with $\alpha_{IIb}\beta_3$ in platelets adherent to fibrinogen immobilized at low and high densities. (A) Western blot analyses of immunoprecipitates obtained from lysates of platelets adherent to fibrinogen immobilized at 2 and 20 μg/mL. Lysates of platelets were subjected to immunoprecipitation with mAb AP3. The proteins in the immunoprecipitates were resolved on SDS–polyacrylamide gels, transferred to the Immobilon P membrane, and probed with anti-skelemin polyclonal (middle panel) and anti-talin (lower panel) monoclonal antibodies. Equal amounts of the β_3 integrin subunit were applied to each well during electrophoresis (upper panel). The coating concentrations of fibrinogen are indicated in the bottom. (B) Densitometry scanning of the immunoprecipitated bands shown in (A). Data are expressed as a percentage of density of protein bands at 20 μg/mL (gray bars) relative to that at 2 μg/mL (100%; black bars). Values are means ± SE of three individual experiments. (C) Western blots showing that the association of talin with the cytoplasmic domain of $\alpha_{IIb}\beta_3$ is induced by adhesion. Western blot analyses of immunoprecipitates obtained from lysates of suspended resting (denoted as "0") and adherent cells (times of adhesion 15–120 min). Lysates of platelets were subjected to immunoprecipitation with mAb AP3. The proteins in the immunoprecipitates were resolved on 7.5%SDS–polyacrylamide gels, transferred to an Immobilon P membrane, and probed with anti-talin and anti-β_3 antibodies. The samples were equalized to contain approximately the same amounts of the β_3 integrin subunit.

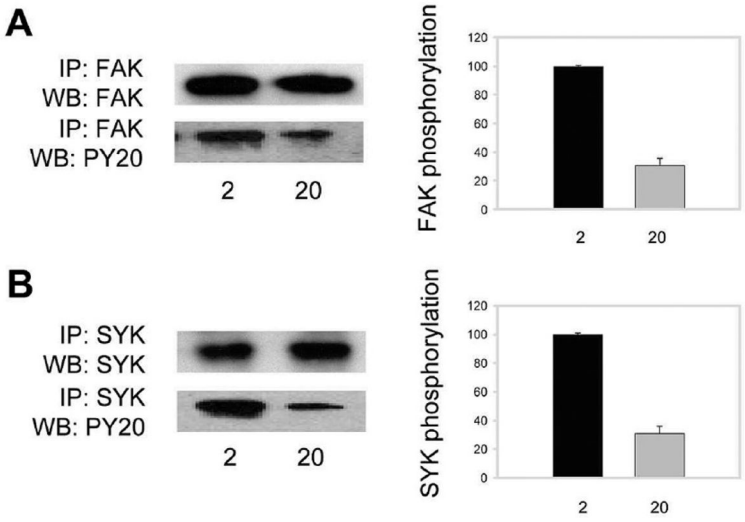

Figure 6.

FAK and Syk phosphorylation in platelets adherent to various fibrinogen matrices. (A, B) Left panels: Platelets adherent to fibrinogen immobilized at 2 and 20 μg/mL were lyzed, and cell lysates were immunoprecipitated with anti-FAK mAb (A) and anti-Syk mAb (B). The proteins in the immunoprecipitates were analyzed by Western blotting using antibodies against total FAK and Syk (upper panels in (A) and (B)) and phospho-Tyr (lower panels in (A) and (B)). Right panels: Densitometry analyses of phosphorylated protein bands. Data are expressed as a percentage of FAK and Syk phosphorylation in cells adherent to 20 μg/mL fibrinogen (gray bars) relative to that to 2 μg/mL (100%; black bars). Values are the means ± SE of three individual experiments.

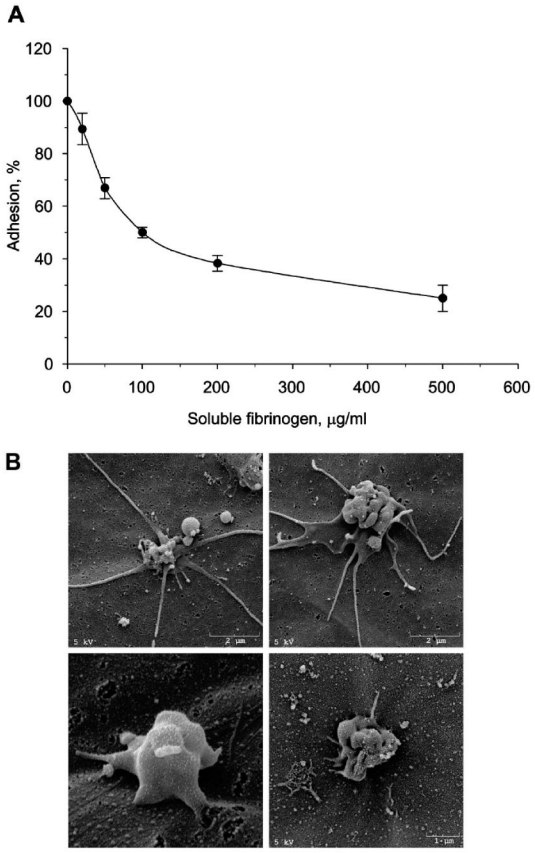

Figure 7.

Effect of soluble fibrinogen on platelet adhesion to the fibrin gel. (A) Fibrin gels were formed in 96-well microtiter plates by mixing 100 μL of 1.5 mg/mL fibrinogen with 0.15 unit/mL thrombin. After polymerization for 2 h at 37 °C, thrombin was inactivated by adding PPACK (5 mM). The gels were incubated with different concentrations of fibrinogen for 30 min at 37 °C, the solution above the gels were aspirated, and the gels were incubated for another 1 h at 37 °C. Aliquots (100 μL) of labeled platelets (1×10^8/mL) were added to each well. After 50 min incubation at 37 °C, the nonadherent cells were removed by two washes with PBS, and fluorescence was measured. Adhesion of platelets to intact fibrin clots (in the absence of fibrinogen)was 16.5±1.2%of added cells. The data shown are the means ± SE of four experiments with triplicate determinations at each experimental point. (B) Scanning electron microscopy of platelets adherent to the naked fibrin gel (upper panel) and to fibrin coated with 1 mg/mL soluble fibrinogen. Fibrin and fibrinogen-treated fibrin gels were prepared as described in Materials and Methods. Two representative platelets adherent to each substrate are shown.

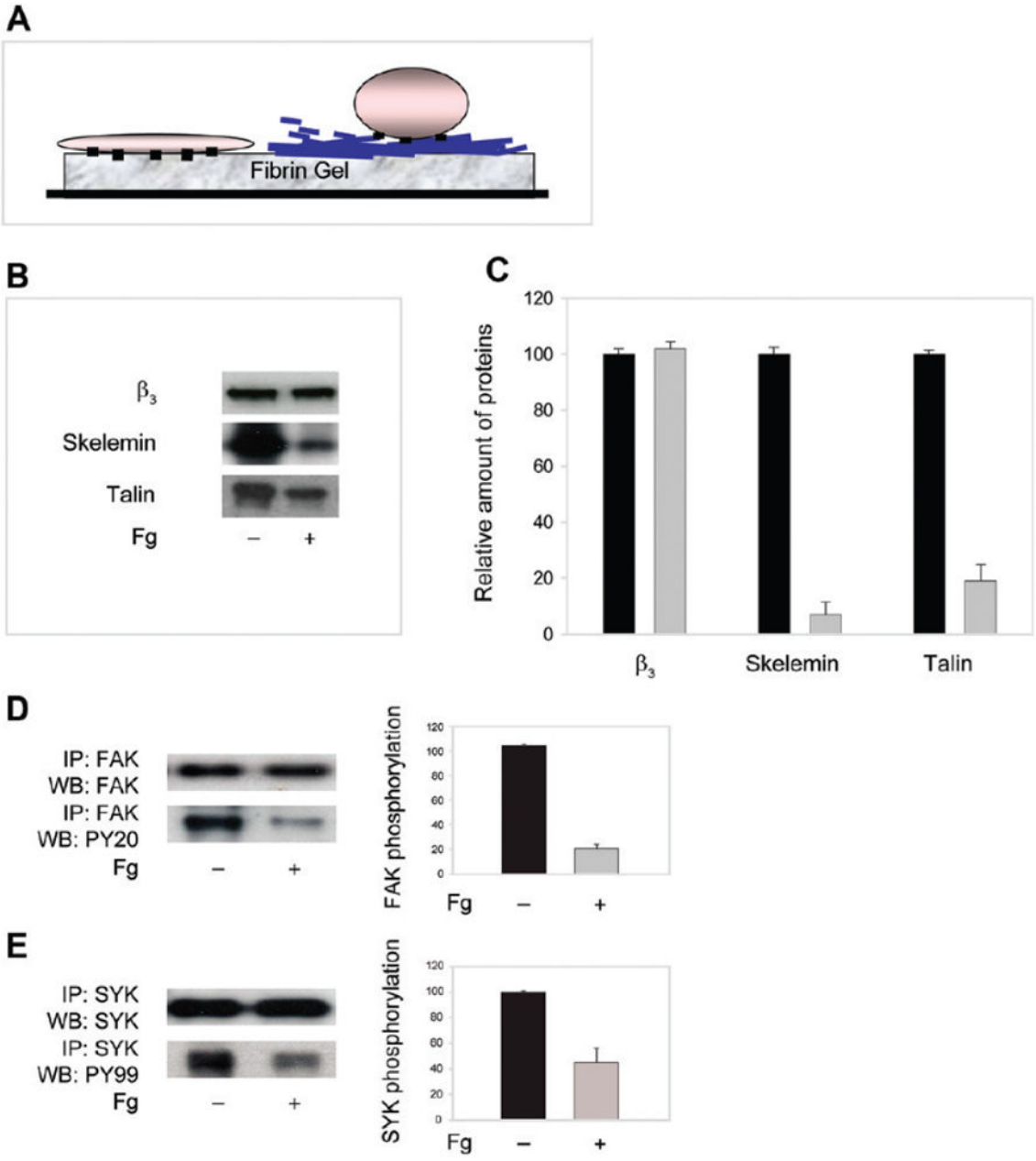

Figure 8.

Differential recruitment of skelemin and talin to $\alpha_{IIb}\beta_3$ and FAK and Syk phosphorylation in platelets adherent to the intact fibrin gel and fibrin coated with soluble fibrinogen. (A) Schematic representation of the surfaces used for cell adhesion. Platelets adherent to the intact fibrin gel (a cell on the left) are spread, while those on fibrin coated with fibrinogen remain round (a cell on the right). (B) Platelets adherent to the intact fibrin gels (−) or gels coated with 1.0 mg/mL soluble fibrinogen (+) were solubilized, cell lysates were incubated with anti-β_3 mAb AP3, and the immunoprecipitated proteins were resolved by SDS–polyacrylamide gel. After transfer to the Immobilon P membrane, the proteins were probed with anti-skelemin (middle panel) polyclonal and anti-talin (lower panel) monoclonal

antibodies. The samples contained equal amounts of the β_3 integrin subunit (upper panel). (C) Densitometry scanning of the immunoprecipitated bands shown in (B). Data are expressed as a percentage of density of protein bands obtained from platelets adherent to fibrinogen-coated fibrin (gray bars) relative to that to the intact gel (100%; black bars). Values are the means and SE of four individual experiments. (D, E) Left panels: Cell lysates of platelets adherent to the intact fibrin gel (−) or to fibrin coated with soluble fibrinogen (+) were immunoprecipitated with anti-FAK mAb (D) and anti-Syk mAb (E), and the samples were analyzed by Western blotting using antibodies against total FAK and Syk (upper panels) and phospho-Tyr (lower panels). Right panel: Densitomety analyses of the immunoprecipitated bands. Data are expressed as a percentage of density of protein bands in the immunoprecipitates from platelets adherent to fibrinogen-coated fibrin (gray bars) relative to that to the intact fibrin gel (100%; black bars). Values are means ± SE of two individual experiments.